Supporting information

Toward a Janus Cluster: Regiospecific Decarboxylation of Ag_{44}(4-MBA)$_{30}$@Ag Nanoparticles

Indranath Chakraborty,[‡] Anirban Som,[‡] Tuhina Adit Maark, Biswajit Mondal, Depanjan Sarkar and Thalappil Pradeep*

Table of contents

List of figures

Computational details

The structure for $Ag_{44}(MBA)_{30}$ utilized in the figures in the main text was generated using the X-ray crystallographic coordinates deposited at the Cambridge Crystallographic Data Centre (CCDC) under the deposition name CCDC 949240. This data is available free of charge from CCDC at http://www.ccdc.cam.ac.uk/data_request/cif.

In this work small model clusters of the type $Ag_1(MBA)_2$, $Ag_1(TP)_2$ and $Ag_1(MBA)_1(TP)_1$ were studied using the Gaussian 09 program package [add ref: Gaussian 09, R. A., M. J. Frish, G. W. Trucks, H. B. Schlegel, G. E. Scuseria, M. A. Robb, J. R. Cheeseman, G. Scalmani, V. Barone, B. Mennucci, G. A. Petersson, et al., Gaussian, Inc., Wallingford CT 2009.].. All calculations were performed using the density functional theory (DFT) method. The Perdew-Burke-Ernzerhof (PBE) exchange-correlation functional[1-2] was used along with along with the Stuttgart/Dresden Effective Core Potentials (ECPs) which included quasi-relativistic effects. The QZVP basis set fitted to the charge density via the W06 fitting set was utilized.[3-4] The following convergence criteria were adopted for the geometry optimizations: 10^{-7} a.u. for energy, 10^{-9} a.u. for electron density, 0.00045 a.u. for force and 0.0018 a.u. for atomic displacement. Absence of imaginary frequencies in the vibrational spectra proved the structures of all the clusters studied herein were real energy minima. The Raman spectra were generated using the visualization program, MOLDEN.[5]

Adsorption of the following species: benzoic acid, benzene, mercapto benzoic acid radical (MBA*) and thiophenol radical (TP*) was studied on Ag(111). These calculations were performed using the python based GPAW code[6] within the atomic simulation environment (ASE).[7] First all the geometries were optimized using the revised Perdew-Burker-Ernzerhof (RPBE) functional[8] and the double zeta polarized (DZP) basis set in the LCAO mode in order to achieve faster computations. Next single point energy calculations were performed with these structures using the van der Waals density functional (vdW-DF2)[9] to obtain accurate adsorption and decarboxylation energies.

The single point energy calculations with vdW-DF2 were carried out with plane-waves. For these plane-wave cut-off energy of 450 eV was employed and the following convergence criteria were used: 0.0005 eV/electron for energy, 0.0001 eV for density and $4.0e^{-08}$ eV^2/electron for eigenstates. The adsorption energies of the adsorbates were calculated with reference to the

corresponding molecules. To this end each molecule was placed at the center of a large unit cell 15 x 15 x 15 Å in dimensions and calculations were performed at the gamma point. For all surface calculations a 4 x 4 x 1 Monkhorst-Pack *k*-point mesh was used and dipole corrections were taken into account. The lattice constant of fcc Ag (bulk) was determined to be 4.22 Å, which was the minimum in the total energy versus lattice constant plot from the LCAO/RPBE calculations. The Ag(111) surface was modeled as a 2 x 4 (atoms) periodic slab four layers thick and with 20 Å of vacuum between neighboring slabs. Of the four layers, the top two were allowed to relax and the bottom two were fixed at their bulk DFT (RPBE)-calculated lattice constant of 4.22 Å. Adsorption of each species (benzoic acid, benzene, MBA* and TP*) was considered at the four unique sites of the Ag(111) surface, namely, on-top, bridge, fcc and hcp.

Figures

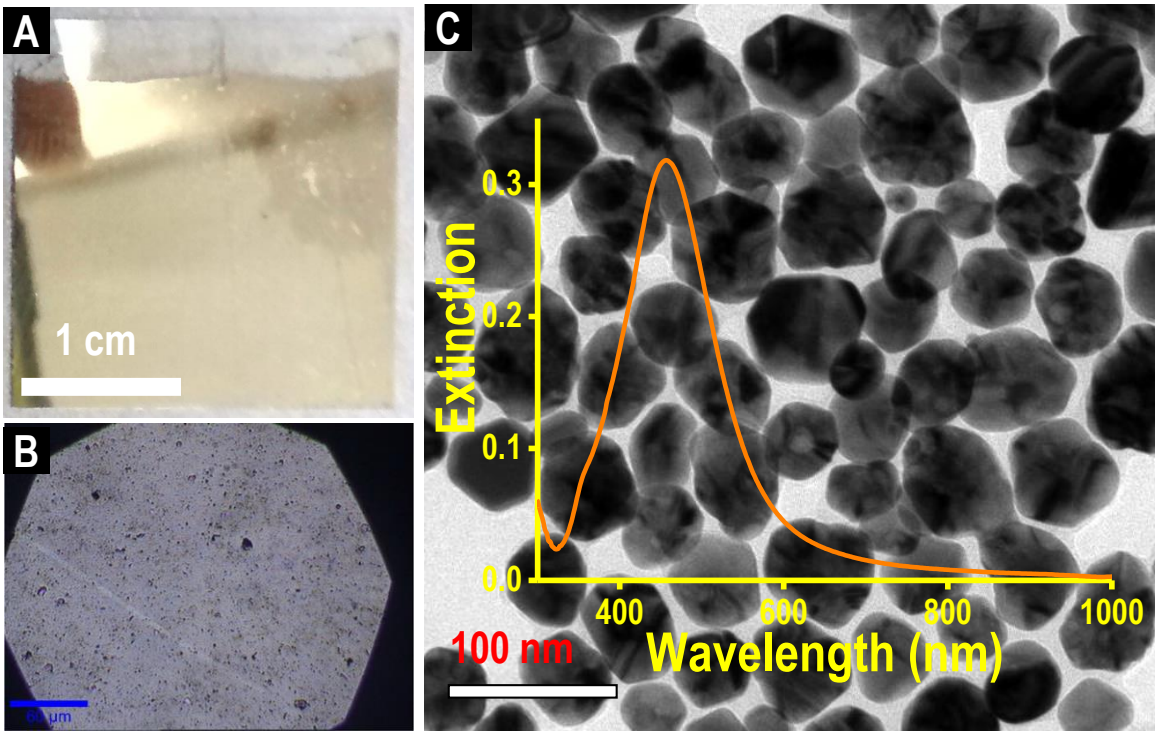

Figure S1: Characterization of silver nanoparticles and the self-assembled monolayer film made on a coverslip. A) Optical image of the nanoparticles film showing shiny golden color. B) and C) TEM image of the self-assembled silver particles. Inset shows the corresponding UV/Vis spectrum of the nanoparticles in solution.

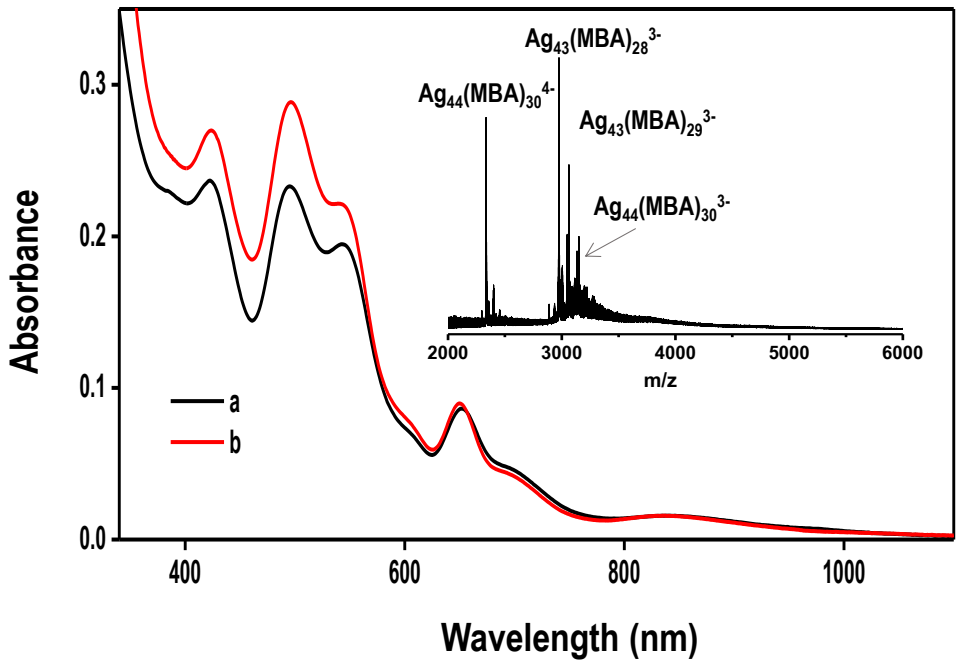

Figure S2: UV/Vis spectrum of the purified $Ag_{44}MBA_{30}$ (a) and $Ag_{44}TP_{30}$ (b) clusters in DMF and acetonitrile solution, respectively showing the characteristic features. The cluster features are indistinguishable from each other. Inset shows the ESI MS spectra of $Ag_{44}(MBA)_{30}$ cluster.

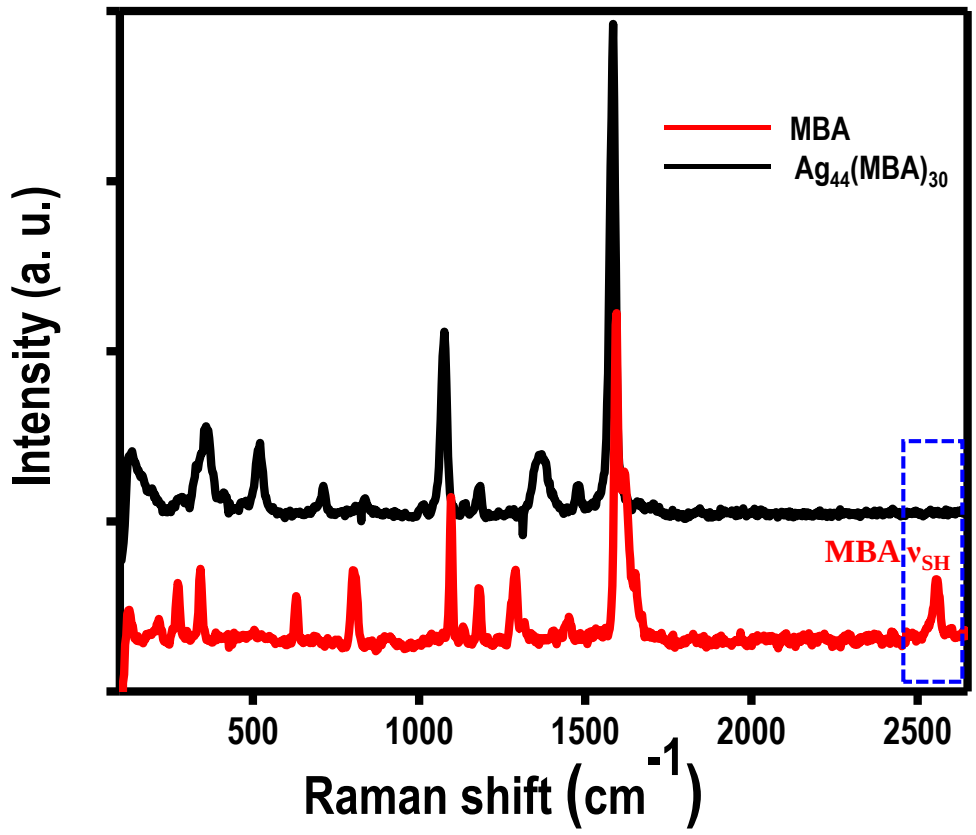

Figure S3: Comparative Raman spectra of $Ag_{44}MBA_{30}$ and MBA. Absence of S-H stretching in $Ag_{44}MBA_{30}$ is marked.

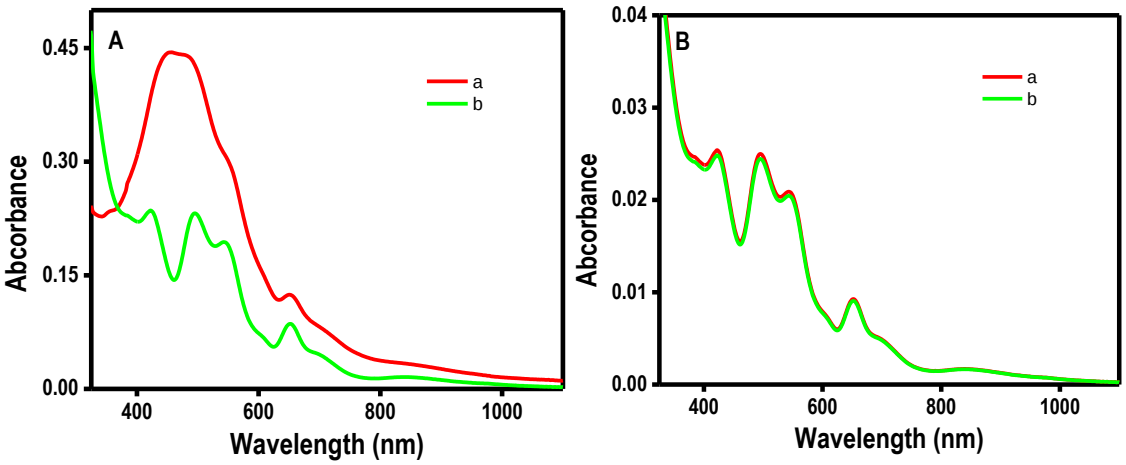

Figure S4: A: (a) UV/Vis spectrum of the solution obtained after extracting $Ag_{44}MBA_{30}$@Ag NPs, post laser irradiation. (b) UV/Vis spectrum of the supernatant solution after centrifugation, showing features corresponding to only Ag_{44}. Ag NPs being bigger in size, precipitated upon centrifugation leaving $Ag_{44}MBA_{30-x}TP_x$ in the solution. This confirms the chemical integrity of the cluster core on Ag NPs upon exposure to the laser beam. B: The UV/Vis spectra of a definite amount of $Ag_{44}(4\text{-MBA})_{30}$ cluster solution before (a) and after (b) before the 633 nm laser irradiation. Very similar absorbance of the cluster solution following laser irradiation confirms the stability of the clusters. Slight decrease in intensity seen is probably due to loss of the clusters during extraction-centrifugation process.

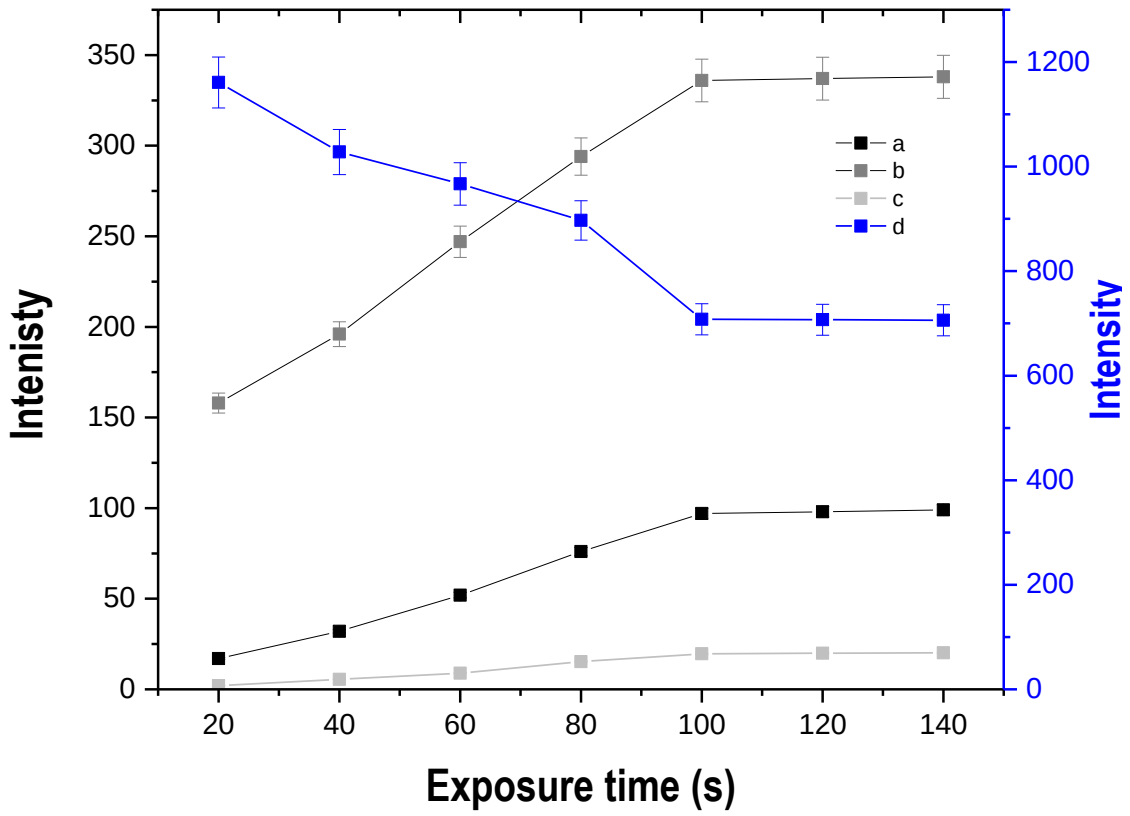

Figure S5: Intensity vs. exposure time plot for the four peaks centered at 1003 cm^{-1} (a), 1026 cm^{-1} (b), 1576 cm^{-1} (c) and 1587 cm^{-1} (d). It is noticeable that for the first three peaks, the intensity increases up to 100 s and then it saturates confirming the end the transformation. The fourth one also follows the same trend but here intensity goes down as it is due to MBA.

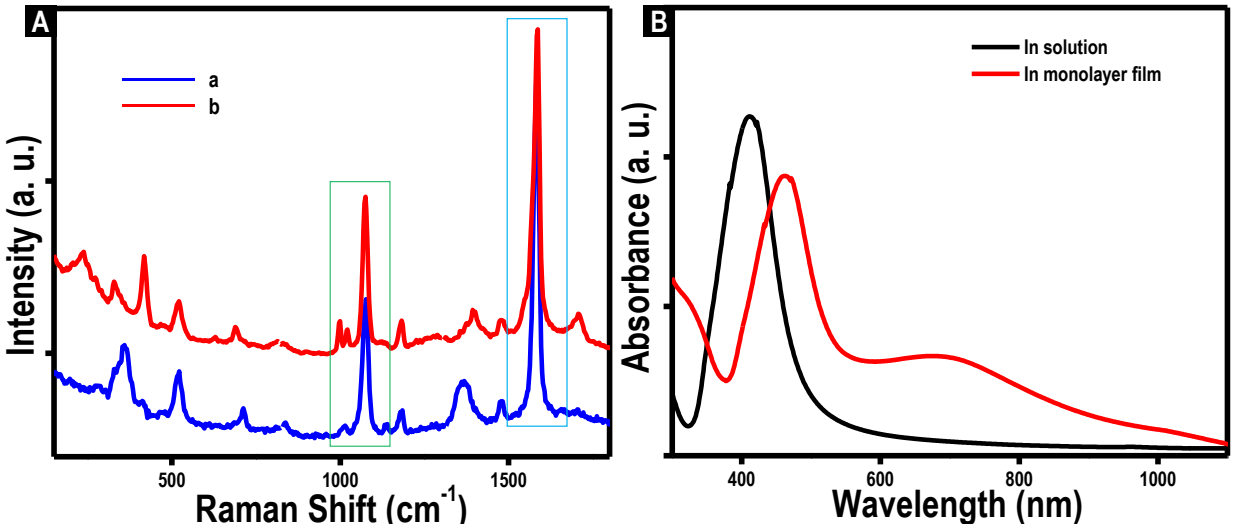

Figure S6: (A) Effect of silver nanoparticles on the decarboxylation. a) Cluster drop-cast on coverslip alone and b) cluster drop-cast on a self-assembled silver nanoparticles film made on a coverslip. Clusters coated on a TLC plate behaved similarly to coverslips. Without silver nanoparticles, decarboxylation did not happen suggesting the effect of plasmon excitation in this process (see the marked regions where the emergence of features due to TP are shown). (B) Difference in the UV-visible spectra of Ag NPs in solution phase with that of a monlayer film transferred onto a microscope cover glass. The film shows signatures of plasmon coupling.

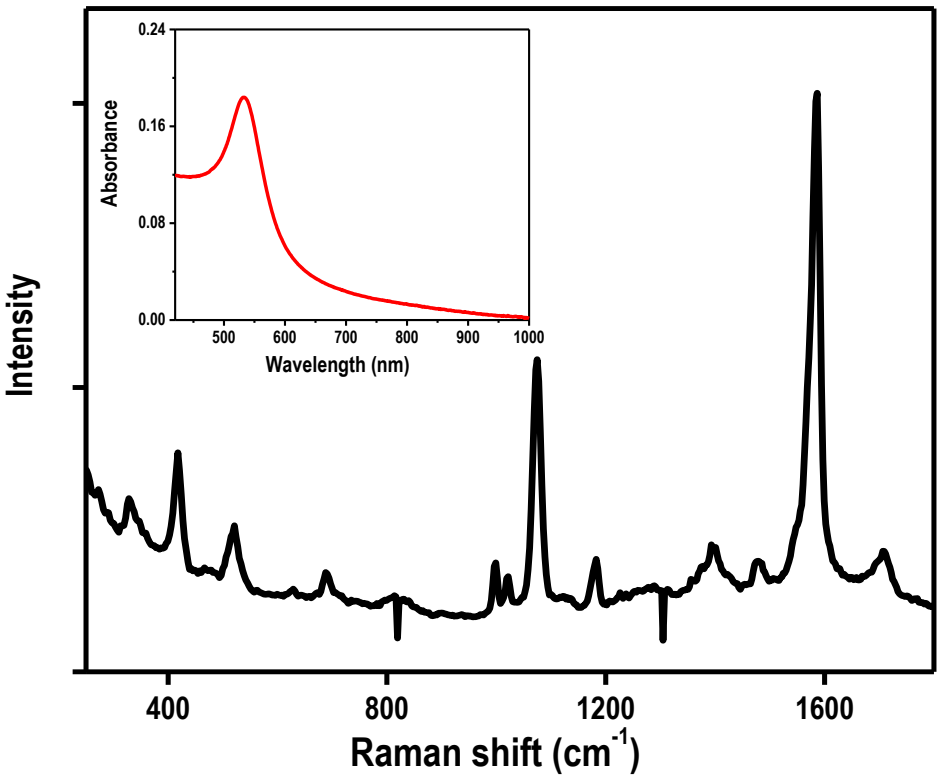

Figure S7: Raman spectrum of $Ag_{44}MBA_{30}$ cluster on a film of Au@PVP. Inset shows the corresponding UV/Vis spectrum of the Au@PVP particle in solution.

REFERENCES

1. Ernzerhof, M.; Perdew, J. P., Generalized Gradient Approximation to the Angle- and System-Averaged Exchange Hole. *J. Chem. Phys.* **1998**, *109*, 3313-3320.

2. Perdew, J. P.; Burke, K.; Ernzerhof, M., Generalized Gradient Approximation Made Simple. *Phys. Rev. Lett.* **1996**, *77*, 3865-3868.

3. Weigend, F., Accurate Coulomb-Fitting Basis Sets for H to Rn. *Phys. Chem. Chem. Phys.* **2006**, *8*, 1057-1065.

4. Weigend, F.; Ahlrichs, R., Balanced Basis Sets of Split Valence, Triple Zeta Valence and Quadruple Zeta Valence Quality for H to Rn: Design and Assessment of Accuracy. *Phys. Chem. Chem. Phys.* **2005**, *7*, 3297-3305.

5. Schaftenaar, G.; Noordik, J. H., Molden: A Pre- and Post-Processing Program for Molecular and Electronic Structures. *J. Comput.-Aided Mol. Des.* **2000**, *14*, 123-134.

6. Enkovaara, J., et al., Electronic Structure Calculations with Gpaw: A Real-Space Implementation of the Projector Augmented-Wave Method. *J. Phys.: Condens. Matter* **2010**, *22*, 253202.

7. Bahn, S. R.; Jacobsen, K. W., An Object-Oriented Scripting Interface to a Legacy Electronic Structure Code. *Comput. Sci. Eng.* **2002**, *4*, 56-66.

8. Hammer, B.; Hansen, L. B.; Nørskov, J. K., Improved Adsorption Energetics within Density-Functional Theory Using Revised Perdew-Burke-Ernzerhof Functionals. *Phys. Rev. B.* **1999**, *59*, 7413-7421.

9. Dion, M.; Rydberg, H.; Schröder, E.; Langreth, D. C.; Lundqvist, B. I., Van Der Waals Density Functional for General Geometries. *Phys. Rev. Lett.* **2004**, *92*, 246401.